





Large-Scale Sequentially-Fed Array Antenna Radiating Flat-Top Beam for Microwave Power Transmission to Drones

NOBUYUKI TAKABAYASHI ¹ (Student Member, IEEE), KATSUMI KAWAI ¹, MIZUKI MASE¹ (Member, IEEE),
NAOKI SHINOHARA ² (Senior Member, IEEE), AND TOMOHIKO MITANI ² (Member, IEEE)

(Regular Paper)

¹Department of Electrical Engineering, Kyoto University, Kyoto 611-0011, Japan

²Research Institute for Sustainable Humanosphere (RISH), Kyoto University, Kyoto 611-0011, Japan

CORRESPONDING AUTHOR: Nobuyuki Takabayashi (e-mail: nobuyuki-takabayashi@rish.kyoto-u.ac.jp).

This work was supported by the Research Institute for Sustainable Humanosphere, Kyoto University, Kyoto, Japan.

This article has supplementary downloadable material available at <https://doi.org/10.1109/JMW.2022.3157845>, provided by the authors.

ABSTRACT Power beaming is one of the core technologies for microwave power transmission (MPT) systems. Effective plane-to-plane power beaming requires not only high point-to-point efficiency but also appropriately-shaped beam to extract the best performance of receivers (rectennas). Flat-top beam plays an important role in plane-to-plane power beaming for drones where the output dc power from rectennas should be maximized to drive motors. It is challenging to develop a large-scale flat-top-beam array with appropriate distribution circuits. Sequential array is also required to suppress axial ratio on the receiving plane. In this paper, we proposed a simplified but effective way to create a large-scale sequential array for flat-top beam at C-band. The series feed and block-oriented sequential array were adopted to keep the circuit design and fabrication simple while obtaining a sufficient point-to-point efficiency and good axial ratio on the receiving plane. A 196-element phased array with microstrip antennas was developed by subdividing the whole array into four 49-element blocks for simplicity of the circuit design and implementation of block-oriented sequential array. The efficiency between the transmitting ports and the receiving ports was 50.6 % in simulations and 32.0 % in measurements. In the measured flat-top beam, the transmitted power was uniformly concentrated within the receiving plane and the axial ratio of the beam was successfully suppressed to less than 3 dB on most of the receiving area. A flight test of a microwave-powered drone was conducted where a micro-drone successfully flew for seven minutes only with wireless power.

INDEX TERMS Drone, flat-top beam, large-scale array, microwave power transmission, sequential array.

I. INTRODUCTION

Wireless Power Transfer (WPT) is expected to play a significant role in a modern society with abundant electrical devices. In 2006, a research group at Massachusetts Institute of Technology performed an innovative WPT experiment involving resonance coupling and revealed that WPT systems were no longer limited to a few centimeters of transmission distance [1]. This discovery kindled zeal of brilliant researchers and engineers for development of various types of WPT technologies such as resonance coupling, microwave power transmission (MPT), laser WPT and so on [2]–[4]. Among those types of

WPT, MPT is perceived as a suitable method for middle- and long-range power transmission. In MPT, power beaming is one of the core technologies because it enables to power electrical devices from several meters to several tens of thousands of kilometers away [5]–[7]. In this research field, the prime focus has been put on increasing point-to-point efficiency and several researchers and research groups theoretically verified that it was possible to increase the efficiency to 100 % with adequate sizes of a transmitter and a receiver in nearfield [6]–[8]. According to [9], “beam collection efficiency exceeding 15 % is only possible if the link distance is less than

the far-field distance of at least one of the two apertures". When W. C. Brown *et al.* achieved the world record of MPT system efficiency (54 %) in 1975, they also put transmitting and receiving antennas closely and generated near-Gaussian beam by the dual-mode horn to obtain more than 90 % of beam collection efficiency [10], [11].

However, the transmitted beams used in those preceding studies were all conventional ones, such as Gaussian beam, focused beam, and beam radiated from a horn antenna. Although those beams are useful to increase point-to-point efficiency to an adequate level, they are missing another important point for an effective power beaming system. The important point is that highly-efficient power beaming is conducted between the plane of a transmitting array and the plane of a receiving array in nearfield. Therefore, it is necessary to more discuss plane-to-plane power beaming for a highly-efficient and practical WPT system. In the plane-to-plane beaming, beam pattern illuminating the surface of a receiving array has to be taken into account in addition to point-to-point efficiency. The beam pattern has a great effect on the availability of maximum dc power and quality of power conversion efficiency (PCE) on rectifiers.

Enhancing output power performance of rectennas (rectifiers and antennas) has been discussed particularly in MPT systems to flying targets because driving dc motors on a flying vehicle consumes a substantial amount of power. Historically, MPT experiments for flying targets have been conducted by several research groups [12]–[14]. In the 1960s, W. C. Brown conducted microwave-powered helicopter experiments with Raytheon, where the helicopter was flown for a continuous period of 10 hours at an altitude of 60 feet with the aid of Gaussian beam and over 4000 rectification diodes [12]. In 1987, a Canadian research group conducted a famous WPT experiment called Stationary High-Altitude Relay Program (SHARP) where a 4.1kg airplane flew with 150W of dc power at 2.45 GHz [13]. In 1992, a Japanese research group conducted MPT experiments for a model aircraft at 2.411 GHz, which is called the Microwave Lifted Airplane eXperiment (MILAX) [14]. In those experiments, researchers tried enhancing the output power of rectennas by expanding the antenna aperture area. This aperture expansion was possible because the aircrafts were prepared only for the experiments. However, the interest in MPT has greatly shifted from experimental aircrafts to practical drones over the last decades [15]–[17]. According to Civil Aviation Safety Authority of Australian Government, drones are categorized into five types depending on its weight [18]. Even the lightest and smallest type of drone (micro-drone) requires more than 20 W of dc power to fly despite that the body size including propellers is typically less than a square of 15 cm [19]. In this case, It is indispensable to extract maximum dc output performance from a limited aperture area of rectennas. Hence it is required to create an appropriately-shaped beam that gives every aperture of antenna elements the maximum radio-frequency (rf) power and extracted the highest dc output power as a whole while maintaining point-to-point efficiency at a high level.

TABLE 1. Summary of Preceding Studies for Flat-Top Beam

Ref.	Freq. (GHz)	Feeding Network	Pol.	Ele. number	HPBW (deg)
[23]	5.8	Microstrip (Series feed)	Linear	6	108
[24]	10.1	Meta surface	N/A	76	Over 34
[25]	1.71 -1.74	Microstrip	N/A	10	Over 40
[26]	1.1 -1.6	Microstrip (Parallel and series feed)	Circular	10	30
[27]	15	SIW leaky-wave	Linear	16	30
This study	5.74	Microstrip (Series feed)	Circular	196	10

In that circumstance, our research group is proposing flat-top beam as a key component of practical MPT systems [20], [21]. The concept of flat-top beam was initially proposed in wireless communication field for the sake of expanding an area of wireless access and ensuring the homogeneous availability of wireless communication in the area [22]. This technology is applicable to power beaming for the purpose of uniform illumination on the receiving plane. We demonstrated that uniform illumination with flat-top beam greatly improved the performance of rectifiers at 2.45 GHz in terms of maximum output power and PCE [21]. In this preceding study, however, there was a fatal problem with plane-to-plane wireless power transmission with flat-top beam. The received pattern of the receiving array was as deformed as the beam no longer functioned as flat-top beam due to the polarization mismatch and the manufacturing errors of the transmitting antenna for flat-top beam.

As seen above, it is necessary to invent a simple and scalable manufacturing method for a transmitting array radiating flat-top beam with good circular-polarization property. Flat-top beam requires specific excitation patterns of amplitude and phase for transmitting elements. Since the excitation pattern of amplitude is similar to sinc-function, power should be unevenly distributed to each antenna [20]. Hence, it is really challenging how to feed signals to antennas with appropriate amplitude and phase for flat-top beam excitation. In Table 1, they are proposing the experimental methods to make flat-top beam [23]–[27].

The abbreviations in the table, Pol., Ele. number, and HPBW respectively stand for polarization, element number, and half-power beamwidth of an array antenna. In [25] and [26], they formed the feeding network with the microstrip-line dividers based on parallel feed. Parallel feed is very useful in terms of isolation between ports. However, this feeding network tends to become too large to integrate the circuit with an array antenna. Moreover, a highly-deviated distribution ratio makes the line width of a $\lambda/4$ impedance transformer impracticably small. In [23], they implemented the feeding network with the microstrip-line divider based on series feed. It contributed to shortening the feed line length and making

the whole circuit compact. However, in this preceding study, a scalable manufacturing method wasn't proposed and as a matter of fact, the element number was 6. In [24], [27], they are respectively introducing metasurface and substrate integrated waveguide (SIW) leaky-wave as feeding networks for flat-top beam. However, those kinds of feeding networks are too complicated to scale up to a large number of phased array. To make a feed network scalable, its design scheme should be simpler. In those preceding studies, the developed arrays have 76 elements at most. A small number of array elements will lead to wide HPBW, which cause a poor point-to-point efficiency due to insufficiency of beam intensity. In the first place, wireless communication focuses to widen the beamwidth for broad communication area while WPT focuses to narrow it for high point-to-point efficiency. For micro-drone applications, the beamwidth is required to be 10 degree, given that a receiver size is a square of 146 mm and a transmission distance is 0.8 m. Therefore, it is indispensable to propose a scalable method to create flat-top beam maintaining a sufficient level of point-to-point efficiency with a large number of elements.

In this paper, we are proposing a scalable and effective method to implement flat beam. We manufactured and measured a 196-element array antenna for flat-top beam excitation. The element number is more than two times as many as those in the preceding studies. The operation frequency of 5.74 GHz was chosen partly because it is included in Industrial, Scientific, and Medical (ISM) frequency band and there are a lot of high-quality microwave components and devices on the market such as solid-state power amplifiers, Schottky barrier diodes and measurement devices. Besides, it has an advantage in compact size of antennas and circuits over 2.45 GHz. For another reason, 5.74 GHz is one of the frequency channels in Japanese new electromagnetic regulations which will be enacted at the end of this year [28], [29]. Those backgrounds drove us to investigate this topic with this frequency band. We're aiming to use the flat-top-beam array developed here for charging a flying drone wirelessly. Therefore, the polarization of this array antenna was designed as circular polarization. It's necessary to create a charging spot for drones in the air where rf power is sufficiently concentrated while keeping axial ratio low.

II. THEORETICAL ANALYSIS OF FLAT-TOP BEAM

Theoretical analysis of beam radiated from a phased array antenna is conducted by (1) to (3), shown at the bottom of the next page, where M, N and k represent a total element number in x -axis, a total element number in y -axis, and wave number in a vacuum, respectively. (x, y, z) and (r, θ, φ) are variables in Cartesian coordinate system and polar coordinate system, respectively. $w_{m,n}$ represents a complex array weight including amplitude and phase information. A calibration factor C is a dimensionless quantity that is required to match a total radiation power with P_T . P_T is a sum of excitation power of all antennas. p_d represents power density at a calculation point (x, y, z) . $F(\theta, \varphi)$ represents a synthesized amplitude component at the calculation point (x, y, z) in nearfield. $E(\theta, \varphi)$ represents

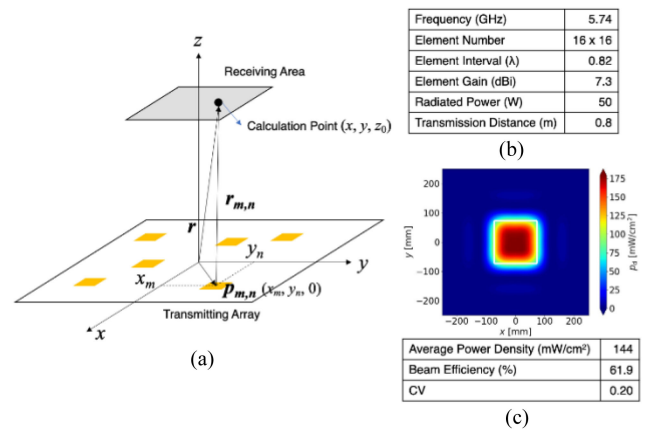


FIGURE 1. Beamforming analysis using Woodward Lawson method. (a) Coordinates and antenna positions for beamforming. (b) Beamforming conditions. (c) Beamforming results of flat-top beam.

an element factor in θ and φ direction. Since $E(\theta, \varphi)$ is the ratio of antenna gain of an element to that of an isotropic antenna, it is a dimensionless quantity. As shown in Fig. 1(a), a transmitting array and a receiving area are put on the planes $z = 0$ and $z = z_0$ with those centers aligned. Since the indices m and n mean array numbers in x -axis and y -axis, the position of the m -th and n -th element is written by a vector $\mathbf{p}_{m,n}(x_m, y_n, 0)$. \mathbf{r} and $\mathbf{r}_{m,n}$ are vectors from the array center to the calculation point and from the m -th and n -th element position to the calculation point, respectively. Note that $r = |\mathbf{r}|$ and $r_{m,n} = |\mathbf{r}_{m,n}|$. In (2), an amplitude component ascribed to the m -th and n -th element is calculated at each calculation point by multiplying $E(\theta, \varphi)$ by $w_{m,n}$, $\exp(-jkr_{m,n})$, and $1/\sqrt{4\pi r_{m,n}}$. $\exp(-jkr_{m,n})$ corresponds with phase change by wave propagation while $1/\sqrt{4\pi r_{m,n}}$ corresponds with amplitude decrement by dissipation of wave. Here, the more accurate $E(\theta, \varphi)$ is, the closer the analyzed p_d gets to practical values. Therefore, the element factor of a microstrip antenna (MSA) was calculated by electromagnetic simulations on CST STUDIO SUITE in advance and the exported element factor was employed as $E(\theta, \varphi)$ in this study. Woodward Lawson method was adopted as a beam design method of flat-top beam [20], [30]. Using this scheme, the beam width of flat-top beam can be adjustable so as to be suitable for a specific application. Since we aim to charge a micro-drone in mid-range with flat-top beam, the conditions of power transmission are given as shown in Fig. 1(b). The transmission distance (z_0) is 0.8 m, the number of transmitting elements is 16-by-16, and the receiving area is a square of 146.4 mm. Fig. 2 shows the calculated power and phase distributions of the flat-top beam array. Using these weights, a two-dimensional beam pattern was calculated as shown in Fig. 1(c). The flat-top beam pattern has 144 mW/cm² and 61.9 % of beam efficiency when the total radiation power was 50 W. The beam efficiency is a ratio of the received power integrated in the receiving area to the total radiation power. Coefficient of variation (CV), which is a ratio of the standard deviation of power density at calculation points to the average, was 0.20. As a reference, CV was calculated as

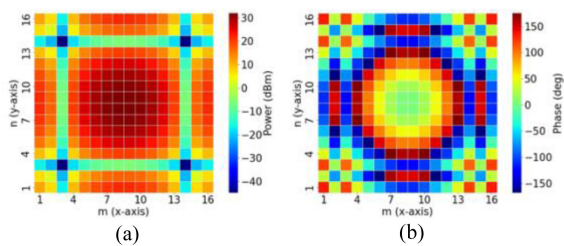


FIGURE 2. Power and phase distributions for the flat-top beam. (a) Heatmap of power distribution (dBm). (b) Heatmap of phase distribution (degree).

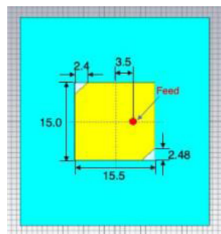


FIGURE 3. Dimensions of a single microstrip antenna for the transmitting array.

0.18 with the array of isotropic antennas when it had the same array weight as in Fig. 2. It means that element factors had less influence on the synthesized pattern than array factors did.

III. SIMULATIONS FOR FLAT-TOP BEAM

A. ELEMENT SIMULATIONS

A phased array antenna that radiates the flat-top beam designed in Section II is simulated in electromagnetic simulations on CST STUDIO SUITE. First, an MSA was designed as an element for a phased array on a dielectric substrate NPC-F260A (1.6-mm thickness) provided by Nippon Pillar Packing Co. Ltd. The relative permittivity and the loss tangent were 2.56 and 0.0015, respectively. As shown in Fig. 3, the two corners of the element were cut off in triangles to make the element right-handed circularly-polarized (RHCP). The reflection coefficient (S_{11}) at 5.74 GHz was -22.6 dB. The boresight gain and axial ratio at 5.74 GHz were 7.3 dBi and 0.34, respectively.

B. ARRAY SIMULATIONS

A 16-by-16-element phased array was modeled in the simulations using the element above, as shown in Fig. 4(a). Following the theoretical analysis in Section II, the element interval

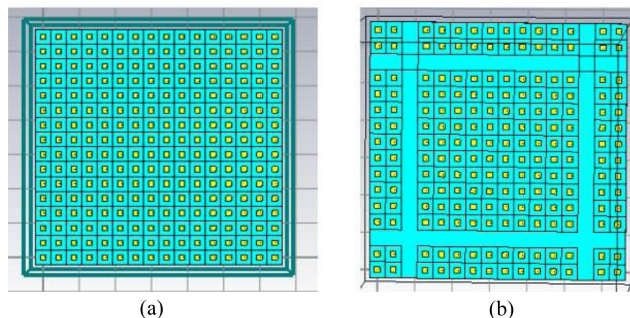


FIGURE 4. Simulation models of the array antennas for flat-top beam. (a) 16-by-16-element array. (b) 14-by-14-element array.

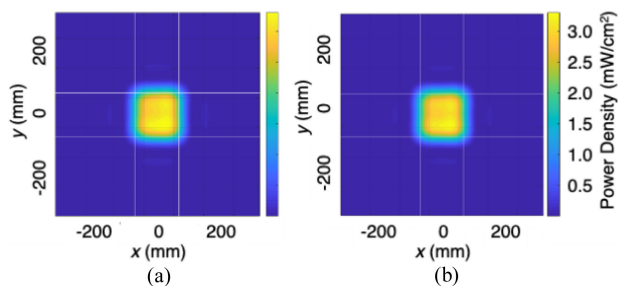


FIGURE 5. Simulated power density of the flat-top beam on the x - y plane ($z = 0.8$ m). (a) Results of the 16-by-16-element array. (b) Results of the 14-by-14-element array.

was set to 0.82λ (42.8 mm). The coaxial components simulating SMA connectors were attached behind the MSAs and signals were excited with waveguide ports where the amplitudes and phases designed in Section II were given. In addition to this model, another array model was prepared for the purpose of exciting the same flat-top beam with fewer elements. In Fig. 2(a), the excitation power levels in the third and fourteenth rows in x -axis and in the third and fourteenth columns in y -axis were more than 30 dB lower than those of the center elements. It is supposed that elements in those lines don't contribute to the consequent radiation pattern of the flat-top beam. Therefore, those elements were eliminated in the second array model as shown in Fig. 4(b). The reduction in element number will make distribution circuit design easier. In the simulations, electrical and magnetic fields radiated from the phased array were monitored on the plane 0.8 m away from the phased array at 5.74 GHz and Poynting vectors were calculated to plot the power density pattern on the receiving plane. In Fig. 5,

$$p_d(x, y, z) = P_T F(x, y, z)^2 \quad (1)$$

$$F(x, y, z) = C \sum_{m=1}^M \sum_{n=1}^N |E(\theta, \phi)| w_{m,n} \exp(-jkr_{m,n}) / \sqrt{4\pi r_{m,n}} \quad (2)$$

$$C = \sqrt{\left(\sum_{m=1}^M \sum_{n=1}^N |w_{m,n}|^2 \int_0^{2\pi} \int_0^\pi |E|^2 d\theta d\phi \right) / \left(\int_0^{2\pi} \int_0^\pi |E|^2 \left| \sum_{m=1}^M \sum_{n=1}^N w_{m,n} \exp(jk\mathbf{p}_{m,n} \cdot \mathbf{r}) \right|^2 d\theta d\phi \right)} \quad (3)$$

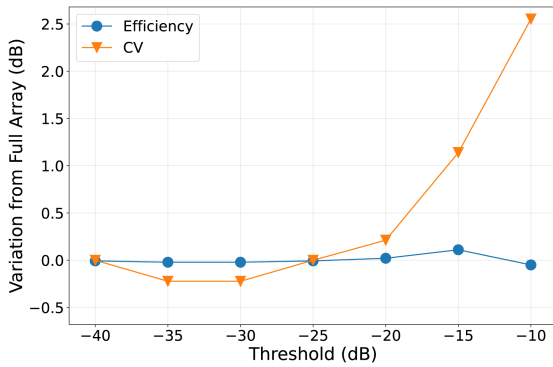


FIGURE 6. Beam efficiency and CV with variable threshold values for element elimination. Each characteristic was plotted as variation from the corresponding value of the full array in Fig. 1.

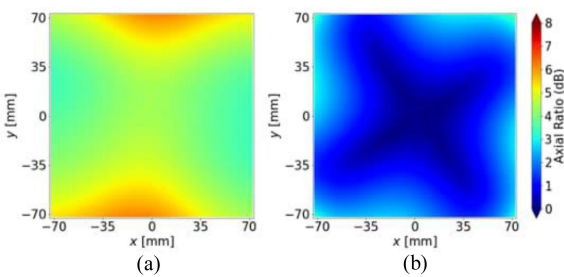


FIGURE 7. Simulated axial ratio on the receiving area (146 x 146 mm) which is 0.8 m away from the transmitter. (a) Results without the proposed sequential array method. (b) Results with the proposed sequential array method.

the power density patterns were compared between the 16-by-16-element array and the 14-by-14-element array when the total transmitted power was 1 W. As shown in this figure, both the beam patterns and the power levels were almost the same between those two. Hence, to simplify the distribution circuit design, the 14-by-14-element array was chosen as the phased array to be developed in the following sections. For wider understanding, the variations of beam efficiency and CV of a radiated flat-top beam were calculated with respect to variable threshold values for element elimination, using (1) to (3). For example, the threshold of -30dB means that elements with the excitation power 30dB less than the peak power were eliminated from the array in Fig. 2. The results are shown in Fig. 6, where the vertical axes were written by ratios to respective values of beam efficiency and CV written in Fig. 1. As the threshold increased, CV gradually became larger while beam efficiency stayed almost the same. It is seen that CV began to increase from the threshold of -20 dB and exceeded 1dB around the threshold of -15dB. Therefore, it can be concluded that the threshold of less than -20 dB was tolerable in this case.

C. BLOCK-ORIENTED SEQUENTIAL ARRAY

Axial ratio in the receiving area was also calculated from the Poynting vectors obtained in the simulations of the 14-by-14-element array in Fig. 7(a). The axial ratio was higher

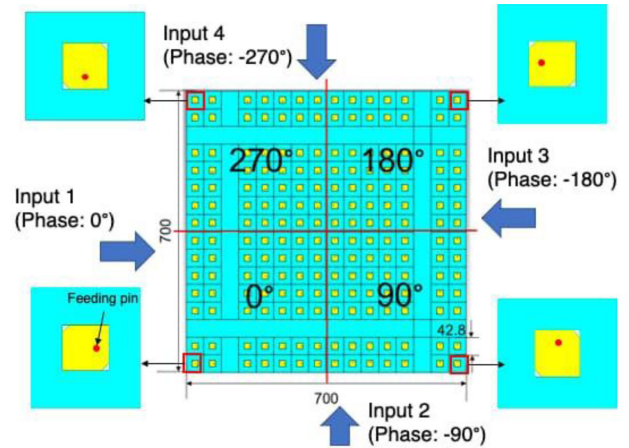


FIGURE 8. Proposed block-oriented sequential array method.

than 3 dB within the entire receiving area (146 mm x 146 mm) despite that the good property of axial ratio was obtained in the element simulations (0.34 dB). Presumably, this deterioration was caused by unfavorable mutual coupling between elements. To improve the axial ratio, sequential array techniques were employed [31]. In the conventional method, each antenna element of an array is physically rotated counterclockwise by 90 degree while the phase of injected signal is electrically delayed by 90 degree in the case of RHCP. These physical and electrical phase rotations enable to cancel the mutual coupling effect while maintaining the beam radiation pattern of the array antenna. However, it is difficult to distribute the appropriate amplitude and phase to each element while considering both of the physical rotation of feeding pins and the electrical phase delays for each antenna element. This requirement makes distribution circuit design incredibly complicated. Hence, we proposed a practical implementation method of sequential array which is shown in Fig. 8. Here, the 196-element array is subdivided into four subarray blocks and each block is rotated counterclockwise by 90 degrees to adjacent blocks, instead of element-by-element rotation. This design method, which we call block-oriented sequential array, makes the distribution circuit design in the following sections far easier. All we have to do is to prepare four pieces of the same 49-way distribution circuit with antennas, to put those pieces on the same plane while rotating them counterclockwise by 90 degrees to each other and to supply four signals with each phase delay (0 degree, -90 degree, -180 degree, and -270 degree) to each block, as shown in Fig. 8. The axial ratio of the sequential array designed with this method is shown in Fig. 7(b). It is confirmed that the axial ratio within the receiving area is suppressed down to less than 3 dB.

IV. EXPERIMENTS FOR FLAT-TOP BEAM

A. 49-WAY POWER DISTRIBUTION CIRCUIT

A 49-way power distribution circuit for radiation of the flat-top beam was fabricated with microstrip lines on a dielectric substrate NPC-F260A (0.6mm) provided by Nippon Pillar

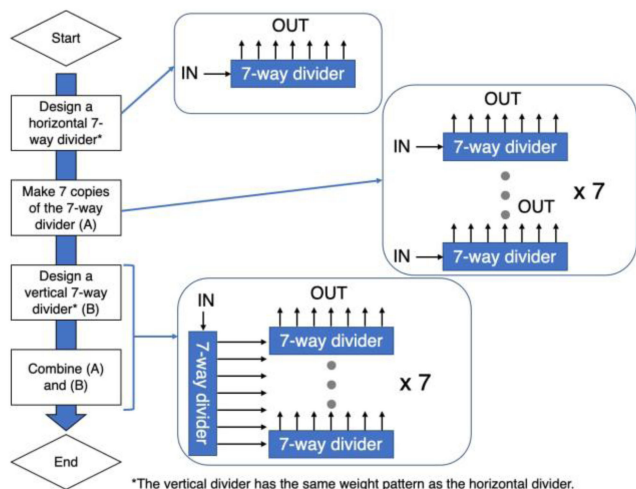


FIGURE 9. Design flow of a 49-way distribution circuit for the flat-top beam.

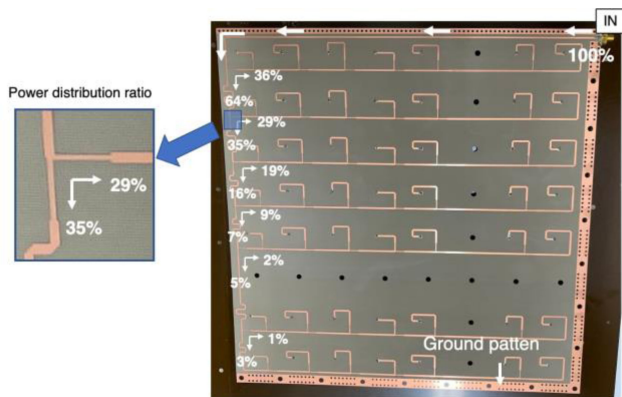


FIGURE 10. Fabricated 49-way distribution circuit. The series feed of microstrip line was adopted and the distribution order was designed in order to reduce the deviation of power distribution ratio.

Packing Co. Ltd. The fabrication flow of the circuit is summarized in Fig. 9. First, a horizontal seven-way divider is designed to distribute the appropriate amplitude and phase to seven antenna elements. Second, this horizontal seven-way divider is copied into seven pieces and those pieces are arranged vertically. Third, a vertical seven-way divider is designed with the same amplitude and phase distribution patterns, but the circuit design is modified in order to connect its seven outputs to each input port of the seven horizontal dividers. Finally, the seven horizontal dividers and the vertical divider are assembled into a 49-way distribution circuit. Since the distribution pattern is symmetric about the x -axis and the y -axis, this distribution flow saves time to design a large-scale distribution circuit. The 49-way distribution circuit fabricated with this flow is shown in Fig. 10. According to the power distribution pattern in Fig. 2, distributed power is concentrated on the center of the whole 196-element array. In Fig. 10, elements located in the upper left require more power than those in the other places. By distributing power to elements requiring higher power in advance of those requiring lower

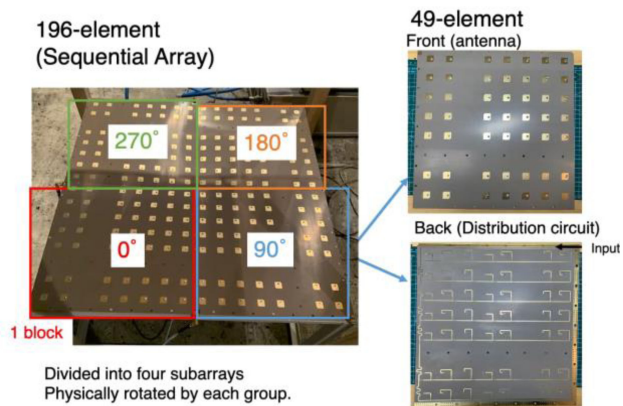


FIGURE 11. 196-element transmitting array antenna for flat-top beam. Four subarrays have antennas and distribution circuits and are placed on the same plane to form a sequential array.

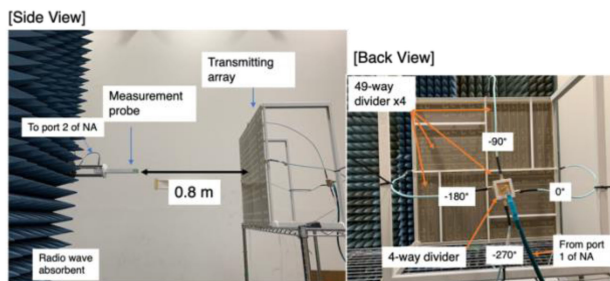


FIGURE 12. Nearfield measurements to obtain the planar power density and axial ratio.

power, the distribution ratio gets smaller as shown in Fig. 10. It is really helpful to avoid the line-width of $\lambda/4$ impedance converters from shrinking to an impracticable size. In addition, the series-fed circuit was adopted to make the whole circuit size compact. The ground patterns were formed on the edges of the substrate to isolate itself from three other 49-way distribution circuits. In the measurement results of the fabricated circuit, the amplitude and phase differences fell within ± 1.5 dB and ± 11 degree, respectively, compared to the designed values in Fig. 2.

B. NEARFIELD MEASUREMENT

A 196-element transmitting array radiating the designed flat-top beam was prepared for WPT experiments, as shown in Fig. 11. The entire array was subdivided into the same four subarray blocks. Those subarrays are rotationally arranged by 90 degree on the same surface for sequential array excitation. Fig. 12 shows the overview of nearfield measurements of the transmitting array. A four-way power divider was prepared and attached before the 49-way power dividers. This four-way divider gives 90-degree phase difference to each block for sequential array excitation. Planar radiation patterns 0.8 m away from the transmitting surface were measured at 5.74 GHz with a measurement probe. After one measurement, this probe physically rotates by 90 degree and remeasures signal level to evaluate signal levels of two polarization axes (x -axis and

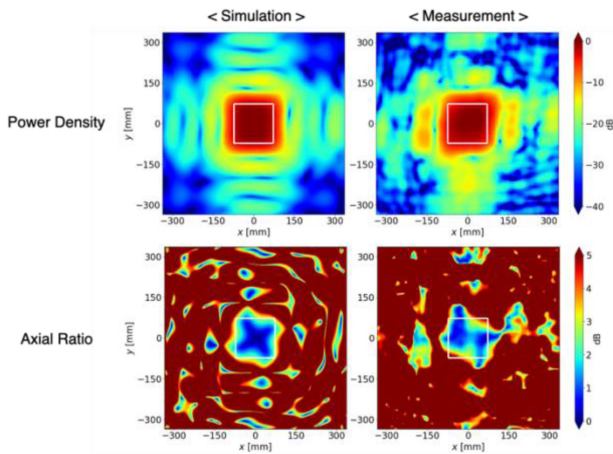


FIGURE 13. Measurement results of power density and axial ratio in nearfield, compared to the corresponding simulation results.

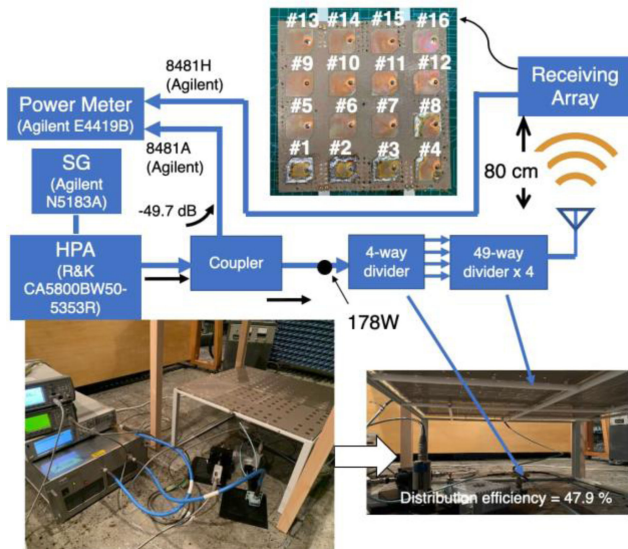


FIGURE 14. Microwave power transmission experiments between the 196-element transmitting array and the 16-element receiving array. The transmission distance was 0.8 m.

y-axis). Fig. 13 shows the results of power density and axial ratio on the measurement plane, in comparison with the corresponding simulation results. The flat-top beam corresponding to the simulation results was successfully radiated from the developed transmitting array in terms of power density and axial ratio patterns. Since amplitude difference within ± 1.5 dB and phase difference within ± 11 degrees were tolerated in the supply circuit design, the measured patterns were a little deformed from the simulated ones.

C. MPT EXPERIMENTS BETWEEN TX AND RX

Fig. 14 shows the measurement setup for power transmission experiments between the 196-element transmitting array (Tx) and a 16-element receiving array (Rx). As shown in this figure, the receiving array having circularly-polarized MSA elements was prepared and numbered as #1 to #16. The received

TABLE 2. Comparison of Received Power on the 16-Element Receiving Array Between the Simulations and the Measurements

Port	Simulation (0.8 m)	Measurement (0.8 m)
Transmitting Element gain	7.3 dBi	7.0 dBi
Total power @ Tx ports	85.3 W	85.3 W
#1 (W)	2.22	1.24
#2	2.80	1.77
#3	2.77	1.63
#4	2.35	1.42
#5	2.57	1.74
#6	3.4	2.08
#7	3.4	1.91
#8	2.74	1.55
#9	2.56	2.00
#10	3.14	2.66
#11	3.24	2.21
#12	2.44	1.48
#13	2.09	1.31
#14	2.56	1.56
#15	2.80	1.49
#16	2.17	1.26
Total power @ Rx ports	43.2 W	27.3 W
Received power density	202 mW/cm ²	127 mW/cm ²
Port-to-port Efficiency	50.6 %	32.0 %
CV	0.15	0.22

rf power of each port was measured on the power meter (Agilent E4419B). The input power was monitored through 49.7 dB attenuated signal with a power sensor (Agilent 8481A). As shown in Fig. 14, rf power at each receiving port was measured with a power sensor (Agilent 8481H) at a distance 0.80 m (15.3λ) away from the transmitter. Input power (P_{in}) was 52.5 dBm (178 W). Power division efficiencies on the four-way power divider and the 49-way power divider were individually measured as 78.6 % and 60.9 % on Keysight Network Analyzer. The total power efficiency and the total power at the transmitting antenna ports were 47.9 % and 85.3 W, respectively. Table 2 shows the measurement results in comparison with the corresponding simulation results.

The operation frequency in both of the simulations and the measurements was 5.74 GHz. Element gain was measured in farfield measurements using two of single MSA elements having the dimensions shown in Fig. 3. Port-to-port efficiency was calculated as a ratio of the total power of all the receiving antenna ports to the total power of all the transmitting antenna ports. The measured value of CV was sufficiently low and close to the simulated value. It is supposed that the slight drop from the simulated value stems from deformation of the measured flat-top beam in Fig. 13. On the other hand, the measured power was substantially lower than the simulated. In Table 3, beam efficiency and CV of the flat-top beam were compared between the theory, the simulations, and the measurements.

TABLE 3. Comparison of Beam Efficiency and CV of Flat-Top Beam Between Theory, Simulations, and Measurements

	Beam Efficiency (%)	CV
Theory	61.9	0.20
Simulation (Non-sequential)	60.7	0.17
Simulation (Sequential)	58.8	0.19
Measurement	37.0*	0.22**

* Obtained by dividing port-to-port efficiency by simulated antenna efficiencies.

** Same value as in Table 2.

Two types of simulation results of non-sequential (Fig. 4) and sequential (Fig. 8) are used here to confirm the difference between before and after sequential arraying. The simulation results didn't include antenna efficiencies of the transmitting array and the receiving array. For the measurements, since it is difficult to measure beam efficiency excluding antenna efficiencies, the beam efficiency was obtained by dividing the measured port-to-port efficiency in Table 2 by the simulated antenna efficiencies of the transmitter (0.91) and the receiver (0.95). The measurement result of CV was the same value as in Table 2. First, the measured CV agreed well with the theory and the simulated. It means that the flat-top beam designed in theoretical analysis was successfully implemented. Next, a 1.2-point difference in beam efficiency between the theory and the simulation result of non-sequential presumably came from mutual coupling effects between antenna elements. Then it dropped by 1.9 points after sequential arraying. The most significant drop occurred between the simulation result of sequential and the measurement result. It is partly because the measured transmitting element gain was 0.3 dB lower than the simulated. If this 0.3-dB drop is taken into account on both of the transmitting side and the receiving side, the measurement beam efficiency is re-estimated as 42.5 %. However, a main reason for the poor beam efficiency is that the measured flat-top beam had higher levels of side lobes than the simulated, as shown in Fig. 13. Although amplitude difference within ± 1.5 dB and phase difference within ± 11 degrees were tolerated in the supply circuit design, those criteria should have been more rigorous to suppress sidelobes and avoid unfavorable energy dissipation.

V. FLIGHT TEST OF MICROWAVE-POWERED DRONE

To test the effectiveness of the developed large-scale array radiating the intensified flat-top beam, the flight test for a micro-drone X400W was conducted with the transmission system shown in Fig. 15. The input power of the transmitting system was enhanced to approximately 280 W with the aid of injection-locked magnetron. Please refer to [32] for the details of the injection-locked magnetron employed. The frequency was set to 5.8 GHz to adjust the operation frequency of the magnetron. Considering the distribution efficiency, 134 W out of 280W from the magnetron system reached the antenna ports in total. Using the same antenna design in Fig. 14, the

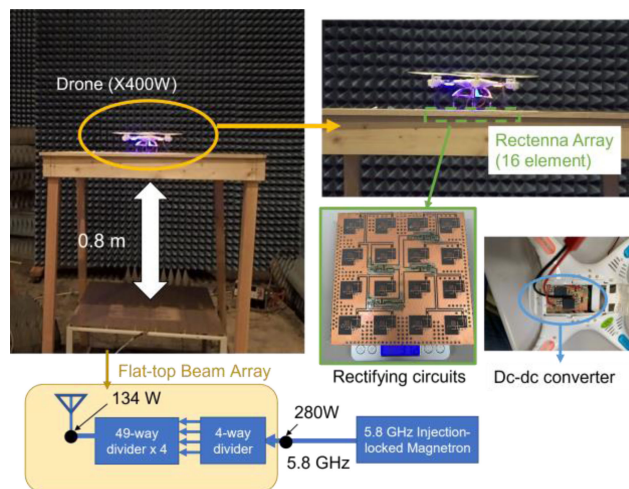


FIGURE 15. Flight test of a microwave-powered drone using the flat-top-beam array developed in the previous section.

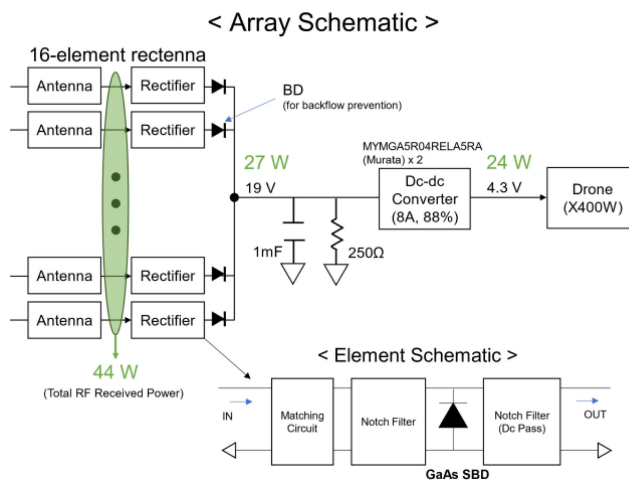


FIGURE 16. Schematics of a 16-element rectenna array and a rectifier element. After rectifiers, a 1 mF capacitor, a 250 Ω resistor, and dc-dc converters are attached for power management.

TABLE 4. SPICE Parameters of Customized GaAs Diode

Ohmic Resistance (Ω)	0.82
Zero-bias Junction Capacitance (pF)	3.0
Breakdown Voltage (V)	60
Junction Potential (V)	0.66
Saturation Current (μA)	6.0
Emission Coefficient	1.63
Grading Coefficient	0.5

receiving system of a 16-element rectenna array was developed with microstrip-line rectifier circuits, GaAs rectification diodes, a dc-dc converter, which consists of two pieces of MYMGA5R04RELA5RA(Murata), and other lumped elements as shown in Fig. 16. SPICE parameters of this customized GaAs diode are shown in Table 4.

A blocking diode TOSHIBA CUHS20S40 for prevention of current backflow was attached at the output of each rectifier. A

smoothing electrolytic capacitor of 1 mF and a resistor of 250 Ω were inserted in shunt after the rectifiers. The resistor was required to avoid a load impedance from being nearly open for rectifiers during a standby period and protect the GaAs diodes before the drone's motors consumed substantial amount of power. In this flight test, the receiving devices except the dc-dc converter were fastened to a wooden frame for stabilizing the power supply. The dc-dc converter was stored in the drone's body. As a result, the drone powered only with wireless energy source successfully kept flying for seven minutes, as shown in Fig. 15.

VI. CONCLUSION

In this paper, the practical method to create flat-top beam for MPT was introduced. Flat-top beam is beneficial to maximize the received power on a receiving antenna while keeping as high efficiency as conventional beams. There are almost no preceding studies which succeeded in making flat-top beam with a large-scale array. The difficulties in creating flat-top beam with a large-scale phased array come from the complexity of making a distribution circuit for the appropriate array weight and the poor quality of axial ratio in the radiated beam. In our proposal, a 196-element phased array radiating the flat-top beam was successfully fabricated. Our proposal includes three main features to make the implementation of flat-top beam radiation easier and scalable. First, array elements having more than 30 dB lower excitation power than the highest power were removable. We confirmed the fact that that removal had almost no impact on the radiation pattern of the flat-top beam through the simulations and the measurements. Second, to make the circuit design simple, the whole 196-element array was divided into four blocks of the same subarrays. It contributes to decreasing the required array number of distribution from 196 to 49. Those four blocks were rotated counterclockwise by 90 degrees when creating the whole array to realize sequential array excitation. It is confirmed that this block-oriented sequential array method greatly contributed to suppressing the axial ratio on the receiving plane. The measured axial ratio in most parts of the receiving area was less than 3 dB. Besides, the design of the 49-way distribution circuit was subdivided into the design of the horizontal and vertical seven-way dividers. Those seven-way dividers had the same array weight as each other but the patterns of microstrip lines were different to fit the whole circuit into a square of 350 mm. Thanks to those methods, we successfully saved the effort of implementing flat-top beam with a large-scale array. Finally, we succeeded in flying a micro-drone for seven minutes only with wireless power from the developed flat-top-beam array antenna. The transmission distance was 0.8 m. Moreover, since our proposed method is scalable, it is applicable to a larger array. Even if the array size grows fourfold (784 elements), the required steps are just making two types of 14-way dividers. It means we can easily extend the transmission distance in drone MPT applications using a larger phased array.

REFERENCES

- [1] A. Kurs, A. Karalis, R. Moffatt, J. D. Joannopoulos, P. Fisher, and M. Soljačić, "Wireless power transfer via strongly coupled magnetic resonances," *Science*, vol. 317, no. 5834, pp. 83–86, 2007.
- [2] R. Hasaba, K. Okamoto, S. Kawata, K. Eguchi, and Y. Koyanagi, "Magnetic resonance wireless power transfer over 10 m with multiple coils immersed in seawater," *IEEE Trans. Microw. Theory Techn.*, vol. 67, no. 11, pp. 4505–4513, Nov. 2019, doi: [10.1109/TMTT.2019.2928291](https://doi.org/10.1109/TMTT.2019.2928291).
- [3] P. Lu, K. Huang, Y. Yang, B. Zhang, F. Cheng, and C. Song, "Space matching for highly efficient microwave wireless power transmission systems: Theory, prototype, and experiments," *IEEE Trans. Microw. Theory Techn.*, vol. 69, no. 3, pp. 1985–1998, Mar. 2021, doi: [10.1109/TMTT.2021.3053969](https://doi.org/10.1109/TMTT.2021.3053969).
- [4] Q. Zhang, W. Fang, Q. Liu, J. Wu, P. Xia, and L. Yang, "Distributed laser charging: A wireless power transfer approach," *IEEE Internet Things J.*, vol. 5, no. 5, pp. 3853–3864, Oct. 2018, doi: [10.1109/JIOT.2018.2851070](https://doi.org/10.1109/JIOT.2018.2851070).
- [5] H. Zeine, "Method & apparatus for focused data communications," U.S. Patent No. 9,351,281, May 24, 2016.
- [6] W. C. Brown and E. E. Eves, "Beamed microwave power transmission and its application to space," *IEEE Trans. Microw. Theory Techn.*, vol. 40, no. 6, pp. 1239–1250, Jun. 1992.
- [7] P. E. Glaser, "Power from the Sun: Its future," *Science*, vol. 162, no. 3856, pp. 857–861, Nov. 1968.
- [8] M. Otsuka *et al.*, "Relation between spacing and receiving efficiency of finite rectenna array (in Japanese)," *IEICE Trans. B-II*, vol. J74-B-II, no. 3, pp. 133–139, 1990.
- [9] C. T. Rodenbeck *et al.*, "Microwave and millimeter wave power beaming," *IEEE J. Microwave*, vol. 1, no. 1, pp. 229–259, Jan. 2021, doi: [10.1109/JMW.2020.3033992](https://doi.org/10.1109/JMW.2020.3033992).
- [10] R. M. Dickinson and W. C. Brown, "Radiated microwave power transmission system efficiency measurements," *NASA Tech. Memo*, pp. 33–727, May 1975.
- [11] W. C. Brown, "The history of power transmission by radio waves," *IEEE Trans. Microw. Theory Techn.*, vol. 32, no. 9, pp. 1230–1242, Sep. 1984.
- [12] Space Studies Institute, "Dr. William Brown wireless power beaming tests," 2017. Accessed: Feb. 23, 2022. [Online]. Available: <https://www.youtube.com/watch?v=9angvvpwH0y8>
- [13] T. W. R. East, "A self-steering array for the SHARP microwave-powered aircraft," *IEEE Trans. Antennas Propag.*, vol. 40, no. 12, pp. 1565–1567, Dec. 1992.
- [14] H. Matsumoto, "Microwave power transmission," *J. Aerosp. Soc.*, vol. 32, pp. 120–127, 1989.
- [15] K. Shimamura *et al.*, "Feasibility study of microwave wireless powered flight for micro air vehicles," *Wireless Power Transfer*, vol. 4, no. 2, pp. 146–159, 2017.
- [16] K. D. Song *et al.*, "Preliminary operational aspects of microwave-powered airship drone," *Int. J. Micro Air Veh.*, vol. 11, 2019.
- [17] R. Moro *et al.*, "28 GHz microwave power beaming to a free-flight drone," in *Proc. IEEE Wireless Power Transfer Conf.*, 2021, pp. 1–4, doi: [10.1109/WPTC51349.2021.9458030](https://doi.org/10.1109/WPTC51349.2021.9458030).
- [18] Civil Aviation Safety Authority, "Types of drones," Australia, 2021, Accessed: Oct. 28, 2021. [Online]. Available: <https://www.casa.gov.au/drones/rules/drone-types>
- [19] DJI, Accessed: Oct. 28, 2021. [Online]. Available: <https://www.dji.com/>
- [20] N. Takabayashi, N. Shinohara, and T. Fujiwara, "Array pattern synthesis of flat-topped beam for microwave power transfer system at volcanoes," in *Proc. IEEE Wireless Power Transfer Conf.*, Jun. 2018, pp. 1–4.
- [21] N. Takabayashi, N. Shinohara, T. Mitani, M. Furukawa, and T. Fujiwara, "Rectification improvement with flat-topped beams on 2.45-GHz rectenna arrays," *IEEE Trans. Microw. Theory Techn.*, vol. 68, no. 3, pp. 1151–1163, Mar. 2020.
- [22] B. Preetham Kumar and G. R. Branner, "Array current distributions to generate flat-topped beams," in *IEEE Antennas Propag. Soc. Int. Symp. Dig.*, 1995, vol. 4, pp. 1810–1813, doi: [10.1109/APS.1995.530936](https://doi.org/10.1109/APS.1995.530936).
- [23] X. Cai, W. Geyi, and Y. Guo, "A compact rectenna with flat-top angular coverage for RF energy harvesting," *IEEE Antennas Wireless Propag. Lett.*, vol. 20, no. 7, pp. 1307–1311, Jul. 2021, doi: [10.1109/LAWP.2021.3078548](https://doi.org/10.1109/LAWP.2021.3078548).
- [24] A. K. Singh, M. P. Abegaonkar, and S. K. Koul, "Wide angle beam steerable high gain flat top beam antenna using graded index metasurface lens," *IEEE Trans. Antennas Propag.*, vol. 67, no. 10, pp. 6334–6343, Oct. 2019, doi: [10.1109/TAP.2019.2923075](https://doi.org/10.1109/TAP.2019.2923075).

- [25] H. J. Zhou, Y. H. Huang, B. H. Sun, and Q. Z. Liu, "Design and realization of a flat-top shaped-beam antenna array," *Prog. Electromagn. Res. Lett.*, vol. 5, pp. 159–166, 2008.
- [26] Z. Zhang, N. Liu, S. Zuo, Y. Li, and G. Fu, "Wideband circularly polarised array antenna with flat-top beam pattern," *IET Microw. Antennas Propag.*, vol. 9, no. 8, pp. 755–761, 2015.
- [27] F. M. Monavar, S. Shamsinejad, R. Mirzavand, J. Melzer, and P. Mousavi, "Beam-steering SIW leaky-wave subarray with flat-topped footprint for 5G applications," *IEEE Trans. Antennas Propag.*, vol. 65, no. 3, pp. 1108–1120, Mar. 2017, doi: [10.1109/TAP.2017.2662208](https://doi.org/10.1109/TAP.2017.2662208).
- [28] N. Shinohara, "History and innovation of wireless power transfer via microwaves," *IEEE J. Microwaves*, vol. 1, no. 1, pp. 218–228, Jan. 2021, doi: [10.1109/JMW.2020.3030896](https://doi.org/10.1109/JMW.2020.3030896).
- [29] Ministry of Internal Affairs and Communications, "Announcement of basic concept of operational coordination to beam wireless power transmission systems and result of appeal for opinions," *Ministry Internal Affairs Commun.*, Japan, 2021. Accessed: Dec. 6, 2021. [Online]. Available: https://www.soumu.go.jp/main_sosiki/joho_tsusin/eng/pressrelease/2021/5/26_02.html
- [30] P. M. Woodward and J. D. Lawson, "The theoretical precision with which an arbitrary radiation-pattern may be obtained from a source of finite size," *J. Inst. Elect. Engineers III, Radio Commun. Eng.*, vol. 95, no. 37, pp. 363–370, 1948.
- [31] J. Huang, "A technique for an array to generate circular polarization with linearly polarized elements," *IEEE Trans. Antennas Propag.*, vol. 34, no. 9, pp. 1113–1124, Sep. 1986.
- [32] B. Yang, N. Takabayashi, T. Mitani, and N. Shinohara, "Wireless power transfer experiment to inflight drone by injection-locking magnetron," *IEICE Tech. Rep.*, vol. 121, no. 290, pp. 28–31, Dec. 2021, (in Japanese).



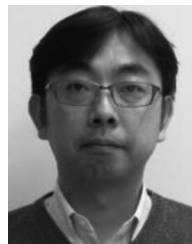
MIZUKI MASE (Member, IEEE) received the B.E. degree in electrical and electronic engineering in 2020 from Kyoto University, Kyoto, Japan, where she is currently working toward the M.E. degree in electrical engineering.

Her research interests include simultaneous wireless information and power transfer and orbital angular momentum multiplexing.



NAOKI SHINOHARA (Senior Member, IEEE) received the B.E. degree in electronic engineering, and the M.E. and Ph.D (Eng.) degrees in electrical engineering from Kyoto University, Kyoto, Japan, in 1991, 1993, and 1996, respectively. In 1996, he was a Research Associate with Kyoto University, where he has been a Professor since 2010. He has been engaged in research on solar power station/satellite and microwave power transmission system. He was an IEEE MTT-S Distinguished Microwave Lecturer during 2016–2018,

and is an IEEE MTT-S Technical Committee 25 (Wireless Power Transfer and Conversion) Former Chair, IEEE MTT-S Kansai Chapter TPC member, IEEE Wireless Power Transfer Conference founder and ExCom committee member, URSI commission D Vice Chair, *International Journal of Wireless Power Transfer* (Hindawi) Executive Editor, the First Chair and Technical Committee member on the IEICE Wireless Power Transfer, Japan Society of Electromagnetic Wave Energy Applications Adviser, Space Solar Power Systems Society Vice Chair, Wireless Power Transfer Consortium for Practical Applications (WiPoT) Chair, and Wireless Power Management Consortium Chair. His books are *Wireless Power Transfer via Radiowaves* (ISTE Ltd. and Wiley) *Recent Wireless Power Transfer Technologies via Radio Waves* (ed.) (River Publishers), and *Wireless Power Transfer: Theory, Technology, and Applications* (ed.) (IET), and some Japanese textbooks of WPT.



TOMOHIKO MITANI (Member, IEEE) received the B.E. degree in electrical and electronic engineering, the M.E. degree in informatics, and the Ph.D. degree in electrical engineering from Kyoto University, Kyoto, Japan, in 1999, 2001, and 2006, respectively.

In 2003, he was an Assistant Professor with the Radio Science Center for Space and Atmosphere, Kyoto University, where he has been an Associate Professor with the Research Institute for Sustainable Humanosphere since 2012. His research

interests include the experimental study of magnetrons, microwave power transmission systems, and applied microwave engineering.

Dr. Mitani is a member of the Institute of Electronics, Information, and Communication Engineers, Japan, and Japan Society of Electromagnetic Wave Energy Applications. Since 2015, he has been a board member of JEMEA. He was the Treasurer of the IEEE MTT-S Kansai Chapter from 2014 to 2017, and has been since 2019.



NOBUYUKI TAKABAYASHI (Student Member, IEEE) received the B.E. degree in electrical and electronic engineering and the M.E. degree in electrical engineering from Kyoto University, Kyoto, Japan, in 2017 and 2019, respectively, where he is currently working toward the Ph.D. degree in electrical engineering.

From 2019 to March 2021, he was an Electrical Engineer with the Department of Product Development, Space Power Technologies, Inc. His works include beamformings and antenna prototyping for

wireless power transmission system used in warehouses and factories.

Mr. Takabayashi was the recipient of the Student Award at 2019 Asia Wireless Power Transfer Workshop and Best Presentation Award at IEEE AP-S Kansai Joint Chapter in 2019.



KATSUMI KAWAI received the B.E. degree in electrical and electronic engineering from the Kobe City College of Technology, Kobe, Japan, in 2019, and the M.E. degree in electric engineering from the University of Kyoto, Kyoto, Japan, in 2021. He is currently working toward the Ph.D. degree in electric engineering.

His research interests include rectenna and wireless power transfer system design.